JOURNAL OF ENERGY SYSTEMS

2024, 8(4)

2602-2052 DOI: 10.30521/jes.1533403 Research Article

Intelligent current-speed soft-starting controller for an induction motor drive system

Amir Abdel Menaem
Mansoura University, Electrical Engineering Department, Mansoura, Egypt, ashassan@mans.edu.eg
Svetlana Beryozkina*
American University of the Middle East, College of Engineering and Technology, Kuwait, svetlana.berjozkina@aum.edu.kw
Murodbek Safaraliev
Ural Federal University, Department of Automated Electrical Systems, 620002 Yekaterinburg, Russia, murodbek_03@mail.ru

Submitted: 15.08.2024
Accepted: 26.12.2024
Published: 31.12.2024

* Corresponding Author

Abstract: In industry, three-phase induction motors (IMs) are the most used motors. IMs' high starting supply current and large accelerating torque make their starting process a potential source of unnecessary energy waste, especially when it is repeated. To overcome the starting problems of an IM, an intelligent soft-starter controller based on an artificial neural network (ANN) is proposed. The controller contains two soft starting control schemes namely, current and speed controls. That allows one to select the soft starting control scheme based on the load requirements and/or supply utility capability. Current and speed controls are to keep the motor's starting current and accelerating torque constant at a specified level, respectively. That is achieved by selecting the appropriate firing angles for the thyristors in the soft starter. The online determination of the thyristor firing angles is resolved through the application of the ANN approach. First, the ANN models for two control techniques are developed using a MATLAB Neural Network Toolbox for training. Based on the current-speed and torque-speed characteristics, two ANN models are trained for a range of thyristor firing angles. Secondly, the ANN models of two control schemes are implemented using MatLab/Simulink for a 3kW three-phase IM. A variety of simulation tests prove that a validation on control technique's effectiveness under various load conditions (no-load, pump, constant, and linear loads) and reference values exists. The least inrush current and smooth acceleration are obtained with two control schemes.

Keywords: *Artificial neural network, AC voltage controller, Current control, Induction motor, Speed control, Soft starter*

Cite this paper as: Menaem AA, Beryozkina S, & Safaraliyev M., Intelligent current-speed soft-starting controller for an induction motor drive system. *Journal of Energy Systems 2024; 8*(4): 221-236, DOI: 10.30521/jes.1533403

2024 Published by peer-reviewed open access scientific journal, JES at DergiPark (https://dergipark.org.tr/jes)

1. INTRODUCTION

Three-phase induction motors (IMs) are extensively utilized in different commercial and industrial applications due to their reliability, robustness, and efficiency [1,2]. However, the starting of IMs have major challenges. Direct-on-line (DOL) starting technique is the cheapest and easiest starting technique. The sudden application of full voltage during motor startup can result in a high inrush current (typically 4 to 7 times the IM rated current) causing thermal stresses on motor bearings, winding, and insulation among windings [3,4,5]. Moreover, these large currents during motor startup can lead to voltage drops in the power supply, particularly if the grid is not robust. It may cause the undervoltage or overload relay to trip, resulting in a supply discontinuity. Therefore, a proper starting scheme is needed to ensure a controlled and smooth motor startup to reduce the inrush current and associated problems for enhancing motor efficiency, extending its lifespan, and reducing maintenance costs [6,7,8,9,10,11,12,13,14,15,16,17].

Reduced voltage starting, electronic reduced voltage starting, and variable frequency starting are the main basic groups employed to start IMs [2]. Initially, the reduced voltage starting method is employed to reduce the high starting current. Star-delta (Y-Δ), autotransformer, and resistor or reactor starting methods are used as reduced-voltage starting techniques to reduce the applied motor voltage [3, 6, 7]. However, this method has several disadvantages such as power losses, frequent maintenance requirements, and potential failure of the moving parts. Secondly, the variable frequency starting method is presented where the starting performance can be regulated by varying the voltage and frequency. Because the variable frequency method requires two converters, it is more costly than the others [8]. To ride these defects, solid-state soft starters are widely used [9].

Soft starters are challenged by operating efficiently over the entire range, but on the other hand they have cost advantages. Recently, the use of inverters has increased in many industrial fields to increase efficiency, but soft starters are still a ubiquitous solution for the starting and braking of induction motors in fixed rotor speed industry applications [18,19]. Soft starters drive not only applications with quadratic load torque behavior, like fans and pumps, but also high inertia applications like circular saws and mills. Not only the improvements of the startup but also the braking of the high inertia loads is an important feature of commercial soft starter products, as high inertias lead to long deceleration times after switching off. Thus, normally passive loads are typical soft starter applications that do not show transients in torque or speed behavior during braking and startup [20]. Even though simple converters for industrial applications, which are also capable of dealing with transients, came onto the market during the last few decades, soft starters are still the preferred solution if speed control brings no advantages in the application. They are very robust and compact and need no additional effort, such as shielded cables or electromagnetic compatibility (EMC) filters. Additionally, their energy efficiency during grid operation is very good due to the bypass contactors, and they are cost-effective compared to comparable simple converters, especially in the rated power range of 1.1–1200 kW [20,21]. Solid-state soft starters use semiconductor devices to regulate the supply voltage applied to the IM during startup. With advancements in semiconductor technology, solid-state soft starters have become more reliable and compact, making them suitable for a wide range of applications. The soft-starter mainly consists of three pairs of thyristors or silicon-controlled rectifiers (SCRs) connected in a series with stator windings of IM. The SCRs can be triggered to gradually increase the motor's voltage during startup [10,11]. Unlike traditional methods such as DOL starting or reduced voltage starting methods, soft starter provides a smooth and controlled ramp-up of voltage and current during motor startup. This results in a gradual acceleration of the motor, reducing stress on the motor and the connected machinery. They offer precise control, smooth acceleration, and reduced starting current. Soft starter adds significant operation flexibility like controlling the acceleration time and reducing the winding heat [12,13]. This flexibility reduces the maintenance cost, increases the mechanical load lifetime, and improves energy efficiency.

Solid-state soft starters come in various types, each designed to cater to specific motor and application requirements [13,14,15,16,17,18,19,20,21]. The choice of the soft starter type depends on factors such as motor size, load characteristics, the initial torque needed, the sensitivity to inrush current, and the level of control required throughout the acceleration process. Based on time functions of firing angle variation [22], solid-state soft starters come in various types. Linear voltage ramp soft starters provide a constant rate of voltage increase over time during motor startup until it reaches the full operating voltage. It is suitable for applications where a simple cost-effective solution is required. Although these voltage ramp techniques are better than the non-electronic starter methods, no more effective current and torque controls are guaranteed during the starting process [23,24,25,26]. Some voltage ramp soft starters combined with control algorithms have been developed. These soft starters incorporate specific control features such as a current-limiting feature along with the voltage ramp [24,25,26]. Closed-loop voltage ramp soft starters incorporate feedback mechanisms to continuously monitor and adjust the startup process based on motor and load conditions. Motor current or estimated torque feedback is needed. In current limiting soft starters, closed-loop control system monitors the motor current during startup and adjust the voltage to precisely limit the inrush current to a predefined level. For the development of closed-loop current limiting soft starters, proportional-integral (PI) and proportional–integral–derivative (PID) controllers have been examined [24,25,26]. A number of adaptive optimization techniques are suggested for the purpose of designing the PI controller ideally, including ACO, GA, PSO, cuckoo search, bat, and flower pollination algorithms [27,28]. To avoid tunning the controller parameters settings, an iterative approach combines the time functions of firing angle change with a mechanism to limit the starting current during motor startup. The firing angle will be reduced depending on the given time function Cosine, exponential, or ramp if the feedback motor current falls below the pre-set current. Otherwise, the firing angle is set constant to restore the current to its pre-set value. The trial-and-error approach has been used to optimize the IM's performance during voltage-controlled soft starting by using alternative time functions for the firing angle of thyristors [22, 24,25,26] or PI controllers [27,28]. In practice, fine-tuning the parameters of the PI controller, presents some challenges, as does selecting the time function of alpha variations through trial and error. Additionally, the motor current's feedback is required.

To avoid the conventional controller difficulties, the soft-starter controller is executed utilizing artificial intelligence (AI) approaches such as artificial neural network (ANN), fuzzy, and adaptive neuro-fuzzy inference system (ANFIS), which is a highly promising instrument in the field of intelligent control [29,30,31,32]. AI based soft starters were employed to change the firing angles in current control methods and torque control techniques [29, 33,34,35,36]. To modify the firing angle depending on motor current deviation and deviation rate, a closed loop fuzzy soft starting controller has been suggested [34]. ANN and ANFIS are used to define the firing angle profile for torque control [29, 35,36]. The estimated motor torque from motor voltages and currents measurements and reference speed profile are combined to determine the firing angle using ANN and ANFIS to maintain a steadily motor speed increase. The controller operates in a closed loop and hence occupy a high number of voltage and current sensors making the control circuit more complex and expensive. Meanwhile, there is no guarantee that the starting current will not exceed the specified value. Furthermore, the motor torque feedback or full parametric definition of the load torque is needed which is very difficult in practice.

In this paper, a simple and reliable soft starter controller using an ANN is developed to overcome the soft starter controller problems. The controller includes two soft starting control techniques: Current control and speed control. Based on the load requirements and/or supply utility capability, the operator can select between the two techniques to meet the industrial requirements of different appliances such as pumps, compressors, fans, blowers, and grinders. In the current control scheme, the ANN model changes the firing angle of thyristors at each motor speed to limit the root mean square (RMS) starting current at the desired reference current. The reference current value is set according to the required limiting value of the motor starting current. In speed control, the ANN model based on the reference speed profile adjusts the firing angle to maintain the accelerating torque at an acceptable level. As a result, the IM has been operating safely with a variety of industrial loads, as there has been no mechanical stress on the drive components.

The paper is organized as follows: Section 2 explains the principle of soft starter operation. Section 3 describes the two models of ANN-based soft-starter control approaches. Section 4 illustrates the modeling of proposed controllers in MatLab/Simulink as well as simulation results. Section 5 discusses simulation results for the proposed control schemes compared with the DOL starting scheme. Section 6 outlines the key findings.

2. OPERATION PRINCIPLES OF SOFT-STARTER FED IM

The soft starter circuit configuration shown in Fig. 1 consists of a set of back-to-back thyristors connected in series with each motor's stator phase windings. Modeling of the series-connected thyristor soft-started IM is found in [37]. The IM is characterized as a combination of RL components and an induced back electric motive force (EMF) source. As became evident in Ref. [38], the IM current is dependent on the EMF and terminal phase voltages. The terminal voltage is controlled by altering the thyristor's alpha concerning the supply voltage's zero crossing. The amplitude and phase of the EMF are determined as functions of motor current and speed. Therefore, the motor terminal phase voltage and the current waveforms change along with the various alpha angles and speeds. The larger the firing angle, the lower the voltage and current, and their RMS values vary according to motor speed. The decrease in the motor speed for a given alpha results in a reduction in the terminal voltage and, therefore, in the current or torque. As a result, the average torque/speed and RMS current-speed characteristic curves of 3 kW IM can be obtained with various alpha angles, as shown in Fig. 2. The motor parameters are given in Table 1. When the alpha is adjusted below its minimum value (θ: the motor's power factor angle), a natural sinusoidal operation occurs. If alpha is increased above the minimal value, the IM begins to operate in a non-sinusoidal mode. Based on the alpha angle, the IM can run in one of three modes: 3-phase, 2-phase, or no-phase.

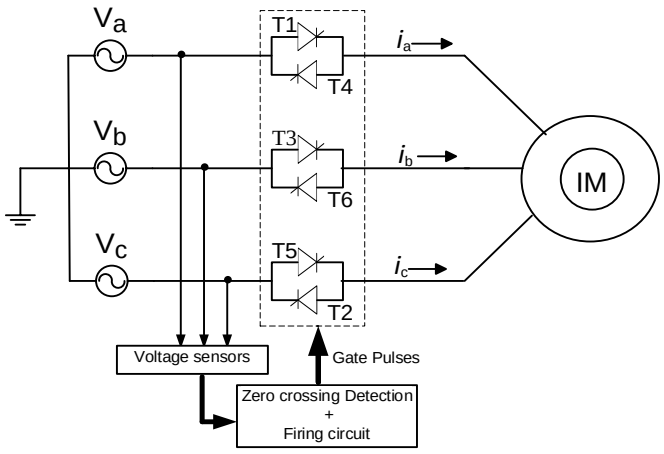

Figure 1. Soft-starter IM derive system.

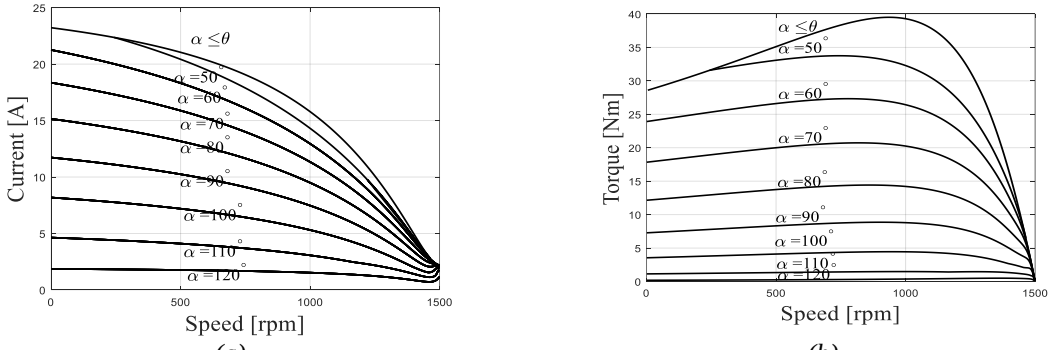

(a) *(b)*

Figure 2. (a) RMS motor current and speed and (b) average torque and speed characteristic curves with various firing angles.

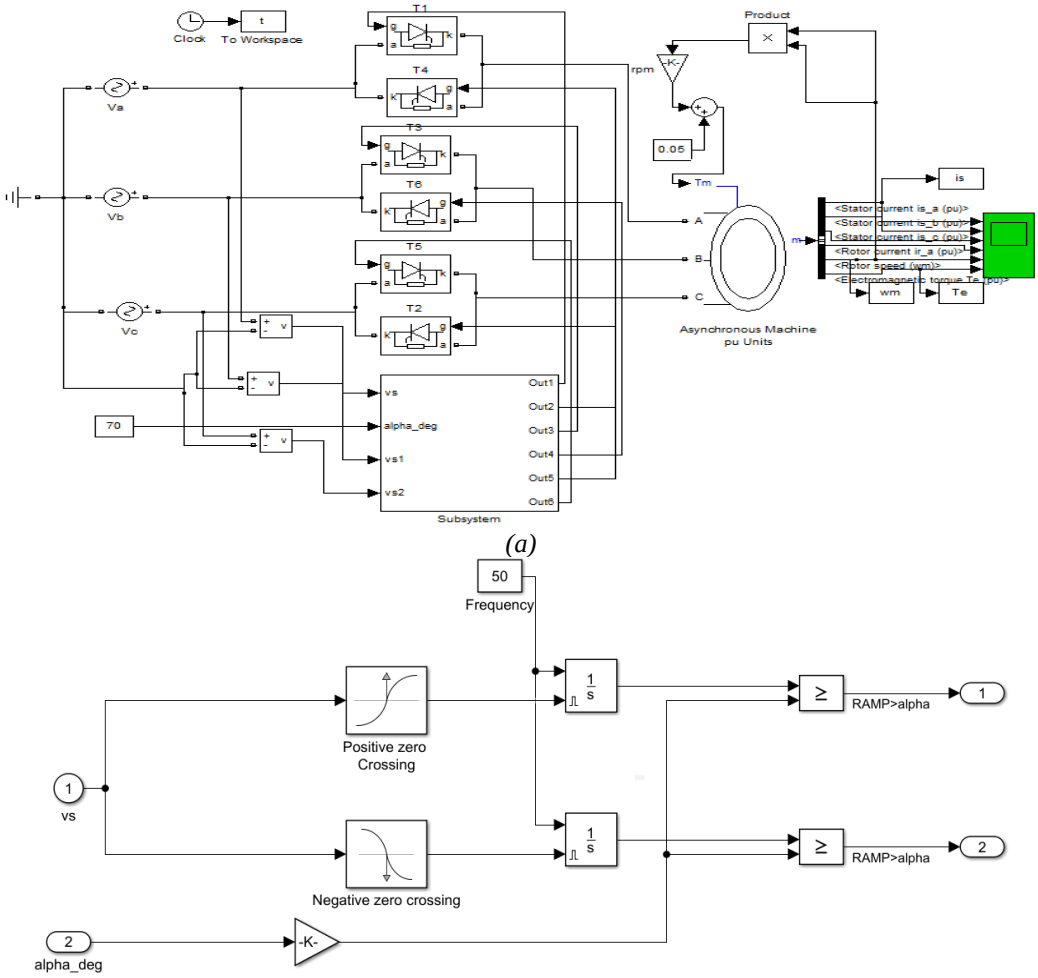

Figure 3. (a) Simulink model of IM derived by soft starter and (b) block model of firing pulses generation for each phase.

Table 1. IM Parameters.

Parameter	Value	Parameter	Value
Rated Power	3 kW	Number of poles	4
Rated frequency	50 Hz	Rated speed	1400 rpm
Rated current- Y/ Δ connected	7.4/ 12.7 A	Moment of inertia	0.034 kg m^2
Rated voltage Y/ Δ connected	380/ 220 V	Stator and referred rotor leakage inductances	0.012 H
Stator and referred rotor resistances	3 Ω	Mutual inductance	0.30 H

3. SOFT-STARTER CONTROLLER BASED ON ANN

To avoid the conventional controller difficulties, the soft-starter controller is executed utilizing an ANN, which is a highly promising instrument in the field of intelligent control. Through learning processes, ANNs gain knowledge and preserve information [39,40]. The ANN strategy is exploited in executing two control techniques, namely the current control technique and the speed control technique. First, a model of IM fed through a soft starter has been developed to study the dynamic performance of a 3-phase IM. MatLab/Simulink simulates the IM with a soft starter system, as illustrated in Figs. 3(a,b). This study deduces the relationships between the RMS line current from the supply and the average developed torque against the motor speed during the starting period at various firing angles of the

thyristors. These IM current-speed characteristic curves presented in Fig. 2(a) are employed during the training procedure of the ANN model to execute the current control technique. While the IM torque-speed characteristic curves presented in Fig. 2(b) are employed during the training procedure of the ANN model to execute the speed control technique.

Two main types of structures are feedforward and recurrent ANNs. In the work, the ANN inputs are the motor's RMS current and speed in the current control approach, as illustrated in Fig. 4. In the speed control approach, the ANN inputs are the motor speed and torque. For both control approaches, the output alpha angle is mostly determined by the current input values and is independent of previous values. As a result, the feedforward ANN is fundamentally convenient to employ.

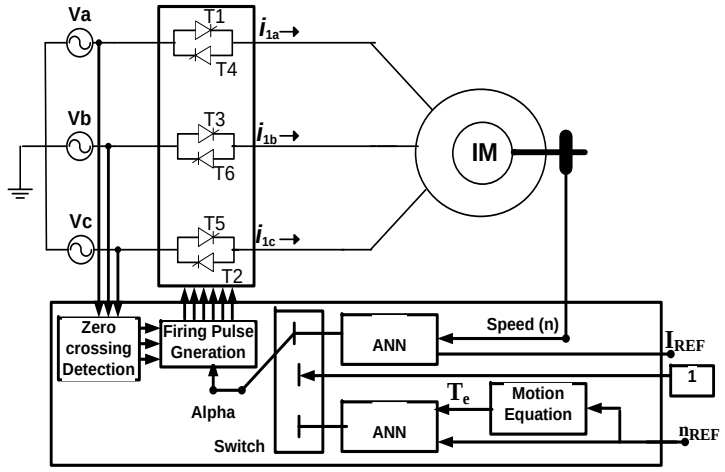

Figure 4. Schematic diagram of soft-starter equipped with the proposed controller.

The feedforward model consists of a single input layer, one or more hidden layers, and an output layer as shown in Fig. 5. Each layer contains a specified number of neurons. The ANN models for two proposed control approaches are developed using the MatLab Neural Network Toolbox. Because there are two inputs and one output, the numbers of neurons in the input and output layers must be set to two and one, respectively. In feedforward models, weights are often adjusted using the back-propagation technique until the mean squared error (MSE) between the actual and reference output patterns is modest. The number of hidden layers and neurons is determined by the problem type and level of precision required. This study uses only one hidden layer. The motor characteristic curves presented in Figs. 2(a,b) are employed during the training procedure. The dataset is randomly partitioned into training, validation, and test sets. 60% of the data is employed for training, 20% for validation, and 20% for testing. To express the nonlinear relationship among variables, the Tan sigmoidal function is the transfer function of the hidden layers, as indicated in Eq. (1). The pure line function represents the output layer's transfer functions as shown in Fig. 5.

$$\varphi(s) = \frac{2}{1 + e^{-2s}} - 1. \qquad (1)$$

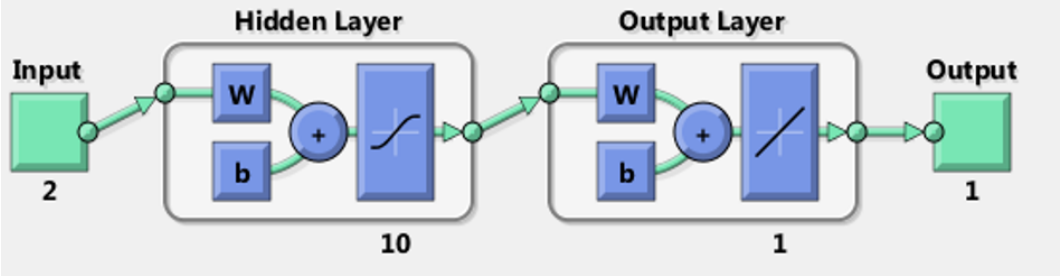

Figure 5. Block diagram of the ANN model.

The ANN configuration for training is created and configured based on the specifications stated in Table 2. The ANN was trained using the Levenberg-Marquardt (LMA) optimization strategy, also known as the back-error propagation algorithm. This method is notable for its high speed and memory requirements [40].

Table 2. ANN configuration parameters.

Parameter	Value
No. of neurons in the input layer	2
No. of neurons in the output layer	1
Training function	Levenberg-Marquardt (trainlm)
Activation function	Tan sigmoidal in the hidden layer and linear in the output layer
Performance goal	0.0001
Maximum training time	15 minutes
Learning rate	0.05

To find the best structure, multiple numbers of neurons in the hidden layer are tested, and the prediction error for each network is computed. Once the desired error objective has been met, the ANN structure is recognized. The LMA algorithm will terminate the training process when one of the following two criteria is met: The training MSE has dropped below the threshold or the maximum training duration has been reached. Following network training, the trained model's performance is tested on a validation dataset, which consists of labeled examples that were not exposed to the model during training. Once the training and validation phases are completed, the testing dataset is utilized to confirm the network's predictive power. After the network's accuracy has been confirmed, the weights and number of neurons in the hidden layer are saved to the prototype ANN in the Simulink model. The training process is terminated when one of the following two criteria is met: Note that the training MSE has dropped below the threshold (0.0002) or the maximum training duration has been reached (20 min). As illustrated in Table 3, the configuration of 10 neurons in one hidden layer achieves the requisite precision (MSE = 0.00011) with a training duration of nine minutes for speed control and seven minutes for current control schemes.

Table 3. Comparison between different ANN structures.

Network Structure	Number of epochs	Mean square error
2-4-1	119	0.0032
2-7-1	307	0.0029
2-10-1	265	0.00011
2-12-1	209	0.00024

To verify the output of ANN models (firing angle), they are tested at different points of inputs (current-torque and speed). The plotting curves in Figs. 6(a,b) use random points to verify the accuracy of the designed ANN models. Figs. 6(a,b) compare the firing angle value, the output of ANN models, with the actual firing angles.The data used in comparison is different from the training data. The results show there is a good fit between the actual and ANN results.

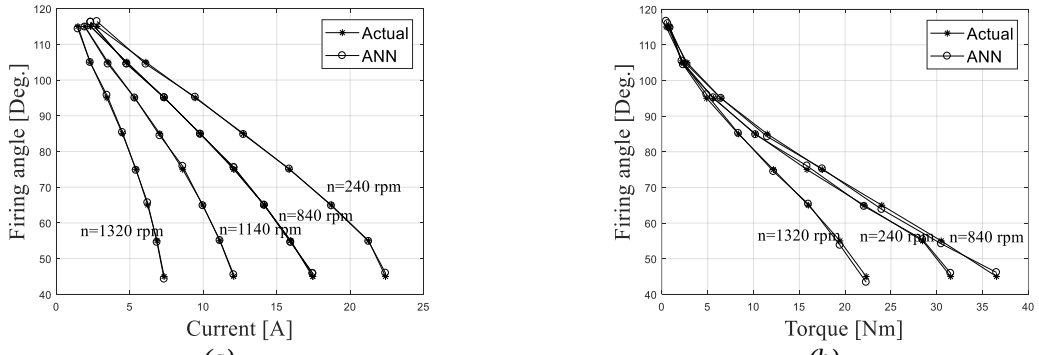

(a) *(b)*

Figure 6. Comparison between the ANN and actual results for (a) current control and (b) speed control schemes.

4. SIMULATION MODEL AND RESULTS

With the parameters of a 3kW IM given in Table 1, the proposed model has been designed and implemented in a MatLab/Simulink media to explore the performance of the proposed soft-starter controller. Both current and speed control schemes are involved in the soft-starter controller. A switch is used to select between the two control schemes, as shown in Fig. 4. MatLab Simulink Power System Blockset and Neural Network Toolbox are used to implement the ANN models and soft-starter-fed IM drive system. Initially, current control technique is used to control the maximum level of the current during startup. Based on IM current-speed characteristic curves, the ANN selects the appropriate firing angle of the thyristors at every point of the motor speed during the starting period in order to maintain the current at the desired level until the motor reaches its rated speed when the thyristors firing angle equals to the power factor angle, i.e., the motor voltage is the same as that of the supply. Secondly, the speed control technique is executed to keep steady ramping of the motor speed during the starting period. Based on IM torque-speed characteristic curves, the ANN adjusts the firing angle of the thyristors at every point of the reference motor speed to whatever value is necessary in order to adapt the developed torque by the motor to the torque profile of the driven load and the desired speed rate to start the motor in the requested time. In the current control scheme, the ANN model generates the alpha angle at each motor speed (n) to restrict the RMS starting current to the required reference current (I_{REF}). The reference current is set to the required motor starting current. In the speed control, the motor torque estimated according to the motion in Eq. (2) is combined with the reference motor speed (n_{REF}) to make the ANN model estimate the alpha angle.

$$T_e = T_L + J\,(d\omega_{REF}/dt) + f\omega_{REF}\,, \qquad (2)$$

where T_L is the load torque, $d\omega_{REF}/dt$ is the motor reference speed change rate (rad/sec^2), f is the friction coefficient, and J is the moment of inertia. To illustrate the benefits of using ANN-based soft starting, DOL starting simulations are also performed. Simulation results for line start and soft start were presented under the following loading conditions:

1) Centrifugal pumps, centrifugal compressors, and blowers' applications are examples of loads for which the load torque varies with the square of the speed.

2) Crushers, elevators, and conveyors are examples of loads for which the load torque is constant over the speed.

Simulation results are presented under the pump loading condition, in which the load torque is equal to $9.3144\text{x}10^{-4}\ \omega_m^2\ Nm$, which develops a mechanical load torque of 20 Nm at the rated speed; constant torque load $T_L = 20\ Nm$, which is full-load torque. Figs. 7(a,d) and Figs. 8(a,d) depict the DOL starting performance of the IM in terms of instantaneous current, RMS current, speed, and electromagnetic torque time responses, while Figs. 9(a,c) and Figs. 10(a,c) depict the motor starting performance with a soft-starter based on the proposed current and speed control schemes under the same load conditions.

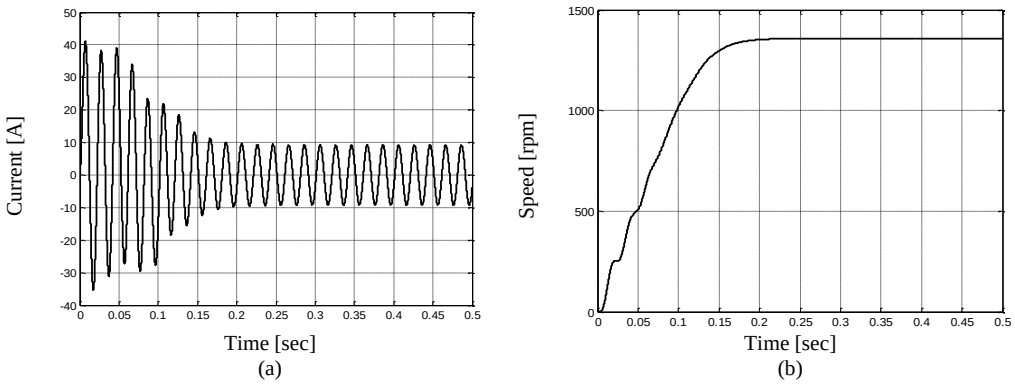

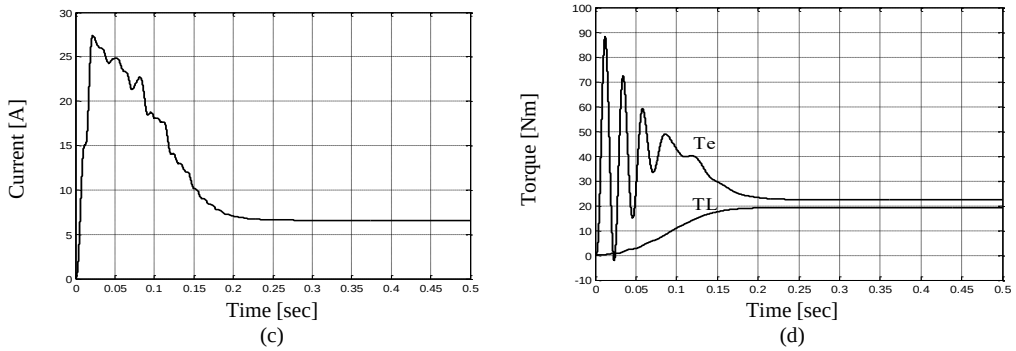

Figure 7. DOL starting performance at pump Load application: (a) Instantaneous current, (b) RMS current, (c) speed, and (d) electromagnetic and load torque time responses.

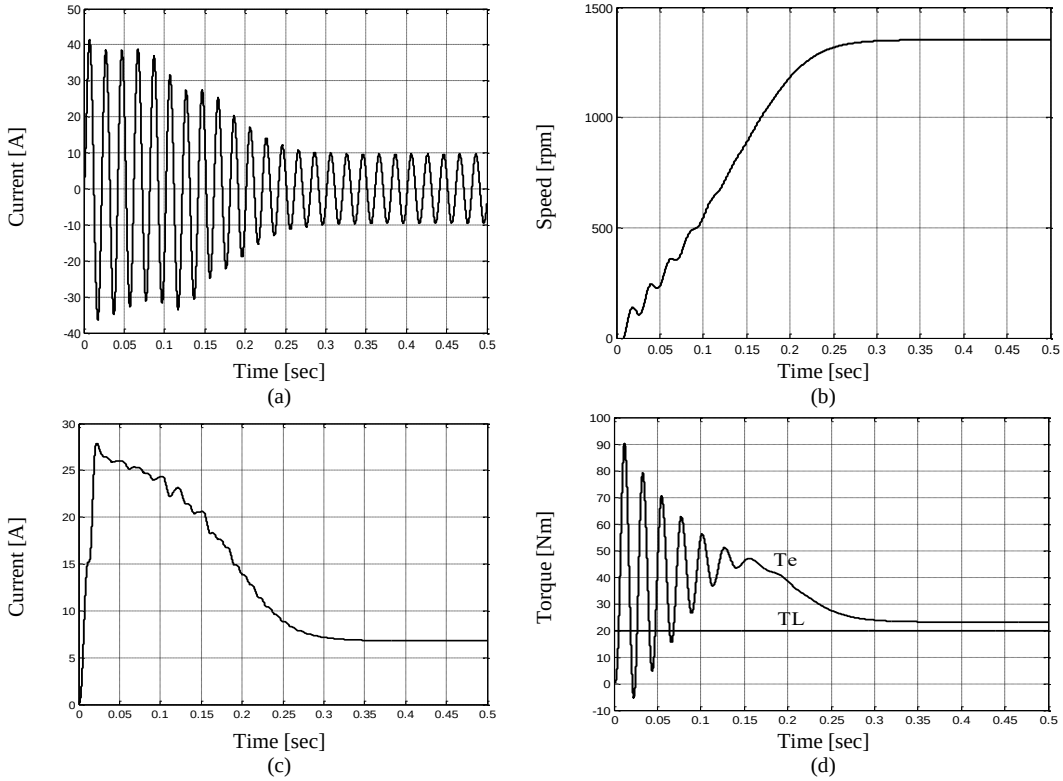

Figure 8. DOL starting performance at constant Load application: (a) Instantaneous current, (b) RMS current, (c) speed, and (d) electromagnetic and load torque time responses.

(a)

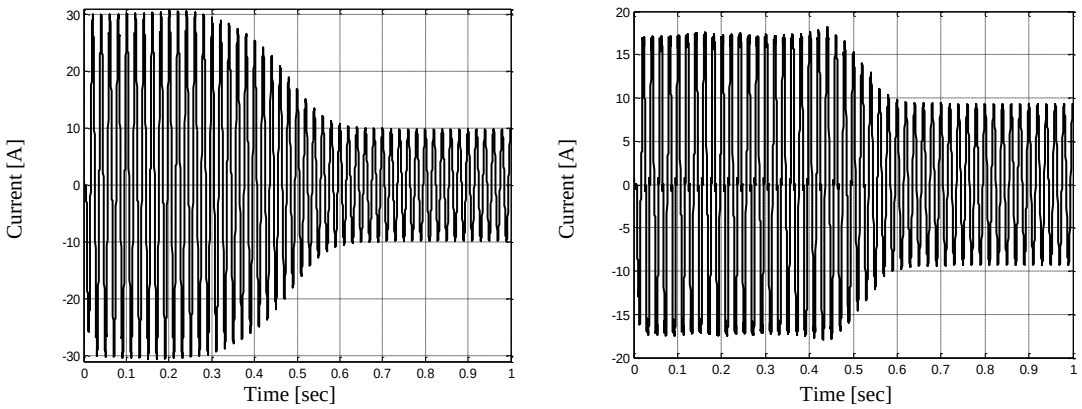

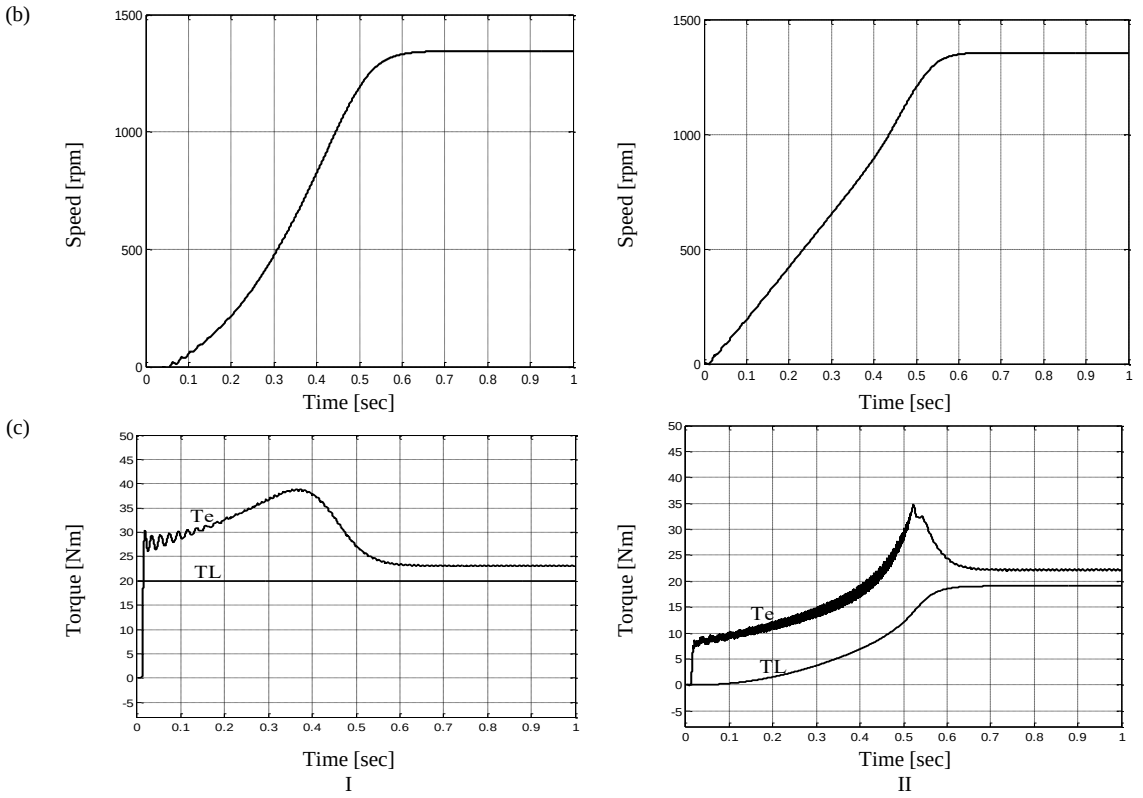

Figure 9. (a) Instantaneous motor current, (b) speed, and (c) torque vs. time for soft-starter with current control scheme at (I) constant load and (II) pump load applications.

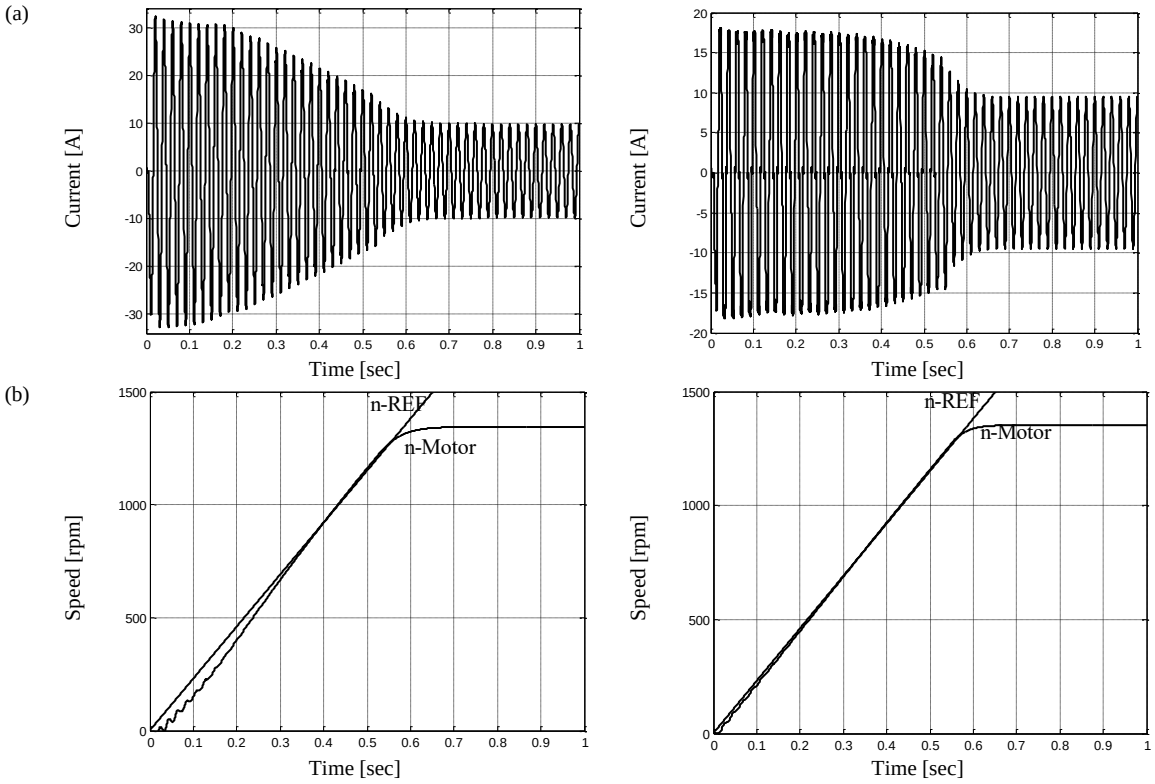

(c)

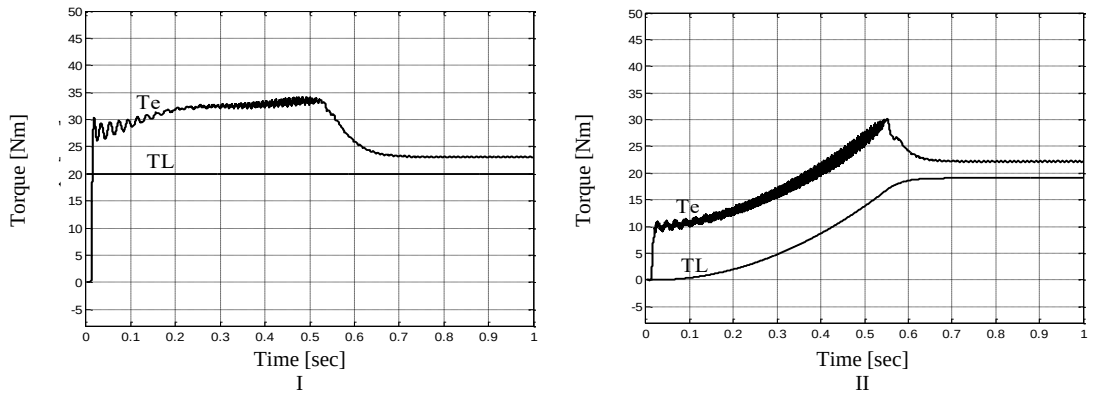

Figure 10. (a) Instantaneous motor current, (b) speed, and (c) torque vs. time for soft-starter with speed control scheme at (I) constant load and (II) pump load applications.

5. DISCUSSION

The results in Figs. 9(a,c) show that the maximum RMS starting current is restricted using the current control scheme at two cases: I) the reference current (13A) for pump load and II) 21A for constant load. While the maximum RMS current of DOL starting is about 27A. In the speed control, the reference speed is set to a linear ramp time function with a rate of 2300 rpm/sec for both pump and constant load applications. The reason behind using ramp increases in speed is to keep the acceleration constant. For comparison between the control techniques, the reference speed is chosen to get the same acceleration time as the current control technique. As shown in Figs. 10(a,c), the speed controller can track the motor speed to the reference value, avoiding the torque pulse observed in the electromagnetic torque profile at the end of the starting time in the case of the current control technique. This pulse is due to the large change in firing angles. However, a higher current level (about 13.7A) for pump load and (23.5A) for constant load has been produced for the speed control scheme.

To study the dynamic performance during starting of IM, the simulation results are compared according to the same factors which are the acceleration time, maximum RMS starting current, load loss factor, and peak positive and negative of the electromagnetic torque. The acceleration time is the time that the motor takes to approximately reach the rated speed of the motor. The power loss caused by resistive or copper losses in the stator windings is dissipated as heat, causing thermal stress to the machine and affecting its upkeep cost and overall lifetime. Since the copper losses are proportional to the square of the current, the load loss factor is considered as in Eq. (3):

$$Loss\ Load\ \ factor = \left(\frac{Maximum\ RMS\ current\ in\ case\ of\ soft-starter\ controller}{Maximum\ RMS\ current\ in\ case\ of\ DOL\ starting}\right)^2 \qquad (3)$$

Finally, the peak positive and negative of the electromagnetic torque is considered as the peak initial of the locked rotor starting torque in the positive and negative direction as it directly relates to mechanical stress on the drive components. The values for these factors under different loading conditions are summarized and given in Table 4.

Table 4. Comparison of simulation results for parametric study.

Type of loading	Type of starting	Acceleration time (sec)	Maximum RMS Current (A)	Loss load factor	+ve/-ve peak torque (Nm)
Pump load	DOL	0.22	27.4	1	88/2
	Current control	0.6	13.3	0.25	10/0
	Speed control	0.6	13.7	0.235	10/0
Constant load	DOL	0.35	27.4	1	88/2
	Current control	0.6	21	0.587	30/0
	Speed control	0.6	23.5	0.735	30/0

Soft-starter reduces the inrush current drawn by the motor, the heating loss factor, and torque pulsations. Both current and speed control schemes can significantly reduce both the starting current and torque pulsations of the DOL technique under pump and constant load applications. This reduction leads to an increase in the acceleration time. They have significant effects on the motor electromagnetic torque during the starting period in which the negative torque pulsation has disappeared and the positive torque pulsation is reduced and consequently the speed build-up is found to be smooth. Using the current control scheme, the maximum RMS current has been reduced to 13.7A under pump load condition and to 21A under constant load conditions with an acceptable increased acceleration time (0.6 sec). While in the speed control scheme, at the same acceleration time and for pump load and constant load conditions, the maximum RMS current has been reduced to 13.3A and 23.5A. Therefore, the current controller can be used to reduce the starting current of the DOL by 51.5% and 23% at the pump load and constant load conditions, respectively. However, using the speed controller, the starting current can be reduced by 50% and 14.5% of the DOL for the pump load and constant load conditions, respectively.

In order to verify the effectiveness of soft-starter controller, simulation results are presented under no-load and linear loading conditions, in which the load torque is equal to 10 Nm at rated speed. Figs. 11(I, II) and Figs. 12(I, II) depict the motor starting performance with a soft-starter based on the proposed current and speed control schemes under different reference currents and speed rates, respectively. Figs. 11(I, II) illustrate the simulation results for the motor stator current, and computed RMS current obtained under current control technique for 12A and 15A current limit at no-load and linear load conditions, respectively. While Figs. 12(I, II) depicts the simulation results obtained for 2350 rpm/sec speed rate at no-load and 1550 at linear load applications. The results have proved the effectiveness and reliability of the control schemes. The results for the proposed current control scheme have indicated that the starting current is nearly kept constant at the reference value during the starting period and reducing the current value increases the acceleration time. It allows one to select a reference current value based on the supply utility capability and the required acceleration time. The results for the proposed speed control scheme have indicated that there is a good tracking between the motor speed and refence values during the starting period under different load conditions and speed rates. Therefore, a smooth acceleration is obtained. It allows one to select a reference speed rate value based on the load requirements.

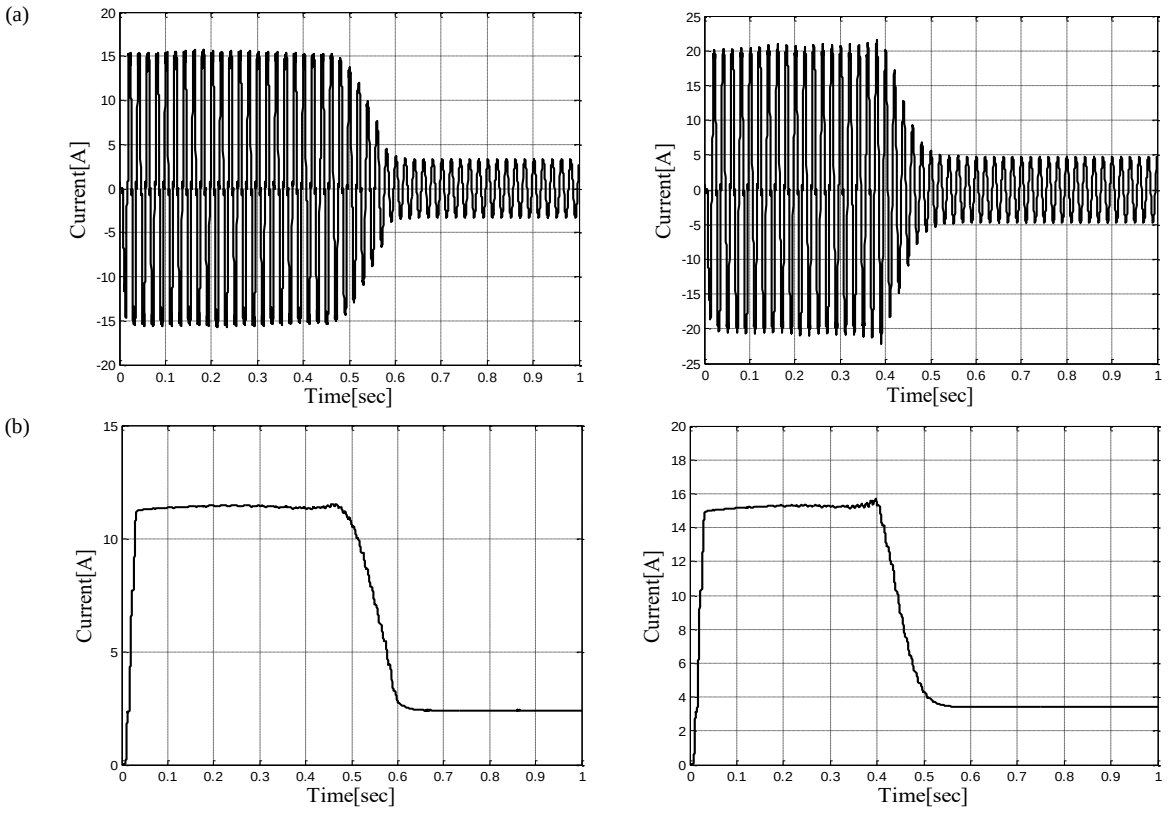

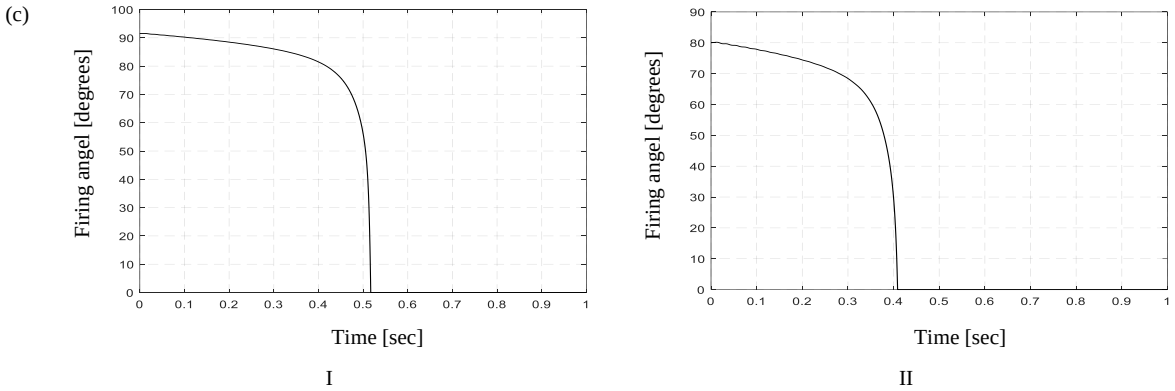

Figure 11. (a) Instantaneous stator phase-a current and (b) its RMS magnitude, and (c) firing angel variation vs. time for soft-starter with current control scheme at (I) no-load application with 12A motor current limit and (II) linear load application with 15A motor current limit.

Table 5 presents some literature works on the control techniques of three-phase IMs. This comparison is based on the art of control, sensor requirements, control algorithm complexity, and the processor cost. The computational complexity of the control algorithm is measured based on the control structure and the computation burden of the control algorithm, i.e., the algorithm's time and memory needed to solve the control problem.

Table 5. A comparison between the proposed soft starter controller and previous works.

Parameters	Control schemes of soft starter			
	[22]	[24,25,26]	[23]	The proposed controller
Control parameter	voltage	current	torque	current/speed
Control type	open loop	closed loop	closed loop	open loop
Sensors count (V: voltage and I: current)	3-V& 3-I	3-V & 1-I	6-V& 3-I	3-V
Firing angle variation	Time function	Time function	PI controller	ANN controller
Algorithm complexity	moderate	moderate	high	low
Cost of the used processor	moderate	moderate	high	low

The soft starting methods presented in literature [22,23,24,25,26,27,28] occupy a high number of voltage and current sensors. Moreover, their control circuits are complicated. The proposed soft starter controller does not require the motor current feedback proposed in [24,25,26,27,28] or the estimated torque feedback proposed in [23]. Only three voltage sensors are needed to detect the zero crossing of the supply voltages in the proposed soft starter controller. Moreover, we have resolved the challenges of tuning the PI controller parameters [27,28] and testing different time functions of firing angle variation [22, 25,26] to achieve the desired performance. Moreover, since the optimal control solution algorithm using the ANN approach is run before the real-time process starts, the control algorithm has become simple. The training data are obtained from the simulink model of the drive and executing the training algorithm offline. Therefore, the low computational burden of a low-cost processor allows for the execution of the control algorithm.

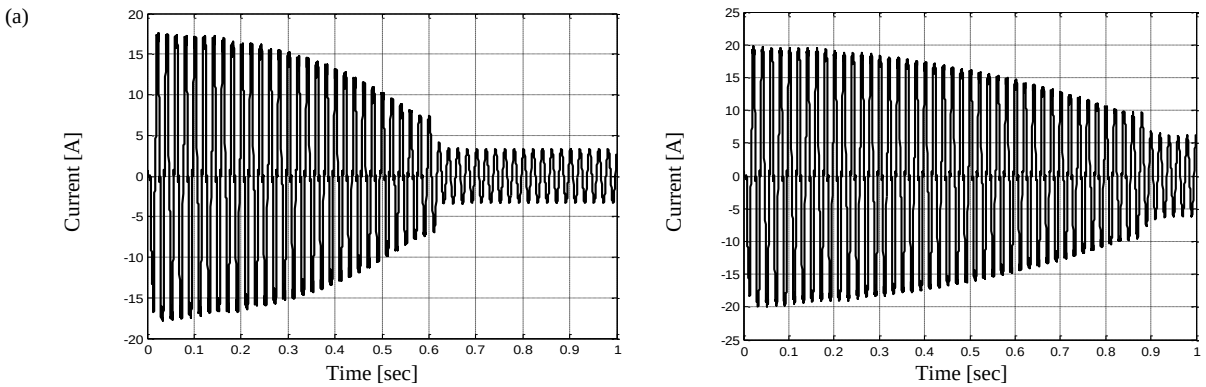

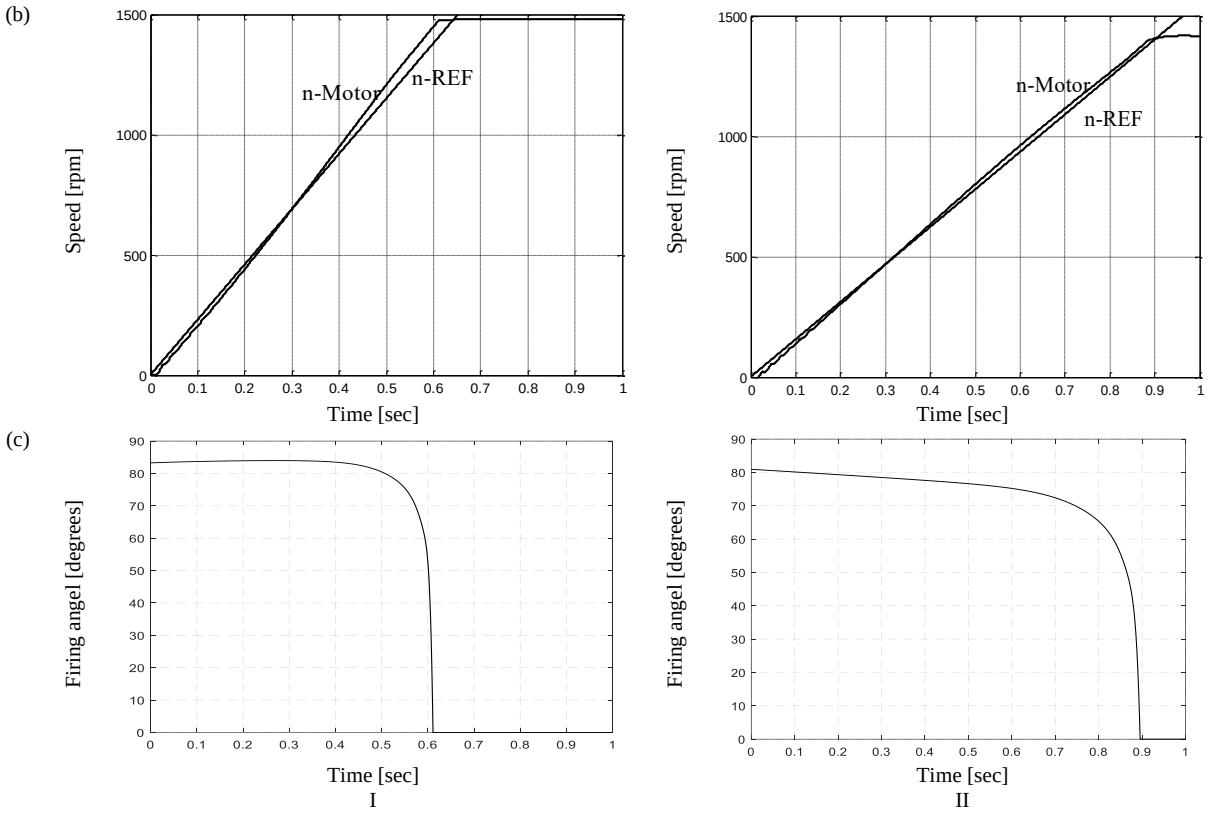

Figure 12. (a) Instantaneous stator phase-a current, (b) motor speed, and (c) firing angel variation vs. time for soft-starter with speed control scheme at (I) no-load application with 2350 rpm/sec reference speed rate and (II) linear load application with 1550 rpm/sec reference speed rate.

6. CONCLUSION

In this paper, the current and speed control schemes for a 3kW 3-phase induction motor that is supplied by a soft-starter are examined based on neural networks. To verify the efficacy of the control schemes under various loading conditions, a sequence of simulation experiments was implemented. The proposed control schemes are demonstrated to be reliable by the results. In contrast to the direct online starting scheme, both control schemes are capable of effectively reducing the maximum RMS starting current and accelerating torque. This allows a smooth start for the IM, reducing mechanical stress on the motor and load couplings and electrical stress on the power source. With an acceptable acceleration time of 0.6 sec under the rated pump load condition, the maximum RMS current becomes nearly 1.7 times the rated current using the current control scheme. While, at the same acceleration time, the maximum RMS starting current is reduced to 1.9 times the rated current by the speed control scheme. However, the torque pulse observed in the electromagnetic torque profile at the end of the starting time in the case of the current control scheme is avoided using the speed controller. Therefore, the current control scheme is more advantageous when the IM is involved in an island microgrid. The speed control scheme is safer than the current control for driving mechanical loads.

REFERENCES

[1] Akbaba M. A novel simple method for elimination of DOL starting transient torque pulsations of three-phase induction motors. *Eng. Sci. Technol. an Int. J.* 2020; 24: 145-157. DOI: https://doi.org/10.1016/j.jestch.2020.06.007

[2] Kłosowski Z, Fajfer M, Ludwikowski Z. Reduction of the Electromagnetic Torque Oscillation during the Direct online (DOL) Starting of a 6 kV Motor by Means of a Controlled Vacuum Circuit-Breaker. *Energies* 2022; 15: 4246. DOI: https://doi.org/10.3390/en15124246
[3] Larabee J, Pellegrino B, Flick B. Induction motor starting methods and issues. In: Record of Conference Papers Industry Applications Society 52nd Annual Petroleum and Chemical Industry Conference; 12-14 Sept. 2005, IEEE, Denver, CO, USA, pp. 217-222.
[4] Pillay K, Nour M, Yang KH, Datu Harun DN, Haw LK. Assessment and comparison of conventional motor starters and modern power electronic drives for induction motor starting characteristics. In: Symposium on Industrial Electronics & Applications; 4-6 Oct. 2009, IEEE, Kuala Lumpur, Malaysia, pp. 584-589.
[5] Liang X, Ilochonwu O. Induction Motor Starting in Practical Industrial Applications. *IEEE Trans. On Industry Appl.* 2011;47:271–280. DOI: https://doi.org/10.1109/TIA.2010.2090848
[6] Knežević I, Ćalasan M, Dlabač T. Novel Analytical Approaches for Induction Machine Direct Start-up Speed–Time Curve Modeling under Fan Load. *Electrical Engineering* 2023; 106: 1925-1938. DOI: https://doi.org/10.1007/s00202-023-02039-3
[7] Jiang F, Tu C, Guo Q, Wu Z, Li Y. Adaptive soft starter for a three-phase induction-motor driving device using a multifunctional series compensator. *IET Electr. Power Appl.* 2019; 13: 977-983. DOI: https://doi.org/10.1049/iet-epa.2018.5079
[8] Chang Y, Yan H, Huang W, Quan R, Zhang Y. A novel starting method with reactive power compensation for induction motors. *IET Power Electronics* 2023; 16: 402-412. DOI: https://doi.org/10.1049/pel2.12392
[9] Malyar V, Hamola O, Maday V, Vasylchyshyn I. Mathematical modeling of starting modes and static characteristics of a wound-rotor induction motor in phase coordinates. *Przeglad Elektrotechniczny* 2023; 10: 114-119. DOI: https://doi.org/10.15199/48.2023.10.22
[10] Huang W, Yuan Y, Chang Y. A novel soft start method based on auto-transformer and magnetic control. In: International Conference on Industrial Technology (ICIT); 14-17 March 2016, IEEE, Taipei, Taiwan, pp. 2108-2113.
[11] Ali A, Erçelebi E. A low-cost modelling of the variable frequency drive optimum in industrial applications. *Journal of Energy Systems* 2018; 2: 28-42. DOI: https://doi.org/10.30521/jes.405774
[12] Hassan A, Amin A, Farahat A. A three-phase induction motor performance under different loading types supplied from balanced and unbalanced Thyristorized supply voltage. *Mansoura Engineering Journal* 2013; 38: 15-39. DOI: https://doi.org/10.21608/bfemu.2020.117181
[13] Tytiuk V, Rozhnenko Z, Baranovska M, Berdai A, Chornyi O, Saravas V. Soft Starters of Powerful Electric Motors and Economic Aspects of Their Application. In: Problems of Automated Electrodrive. Theory and Practice (PAEP); 21-25 Sept. 2020, IEEE, Kremenchuk, Ukraine, pp. 1-4.
[14] Kosykh E, Udovichenko A, Lopatkin N, Zinoviev G, Grishanov E, Sarakhanova R. Analysis of the Control System for a Soft Starter of an Induction Motor Based on a Multi-Zone AC Voltage Converter. *Electronics* 2022; 12:56. DOI: https://doi.org/10.3390/electronics12010056
[15] Wang Y, Yin K, Yuan Y, Chen J. Current-Limiting Soft Starting Method for a High-Voltage and High-Power Motor. *Energies* 2019; 12:3068. DOI: https://doi.org/10.3390/en12163068
[16] Furtsev NG, Petrikov AS, Belyaev AN. Optimizing Soft Starter Algorithms for Heavy Induction Motors to Ensure Stable Operation of Autonomous Power Systems. In: Conference of Russian Young Researchers in Electrical and Electronic Engineering (EIConRus); 27-30 Jan. 2020, IEEE, St. Petersburg and Moscow, Russia, pp. 1222–1226.
[17] Sharifian M, Feyzi M, Sabahi M, Farrokhifar M. A new soft starting method for wound-rotor induction motor. *Journal of Electrical Engineering* 2011; 62:31–36. DOI: https://doi.org/10.2478/v10187-011-0005-3
[18] Simms S, Gabriel T, Thomas A. Novel voltage observer for reduced voltage soft-starter torque ramp: description and analysis results. *IEEE Industry Applications Magazine* 2023; 29:24–32. DOI: https://doi.org/10.1109/MIAS.2023.3285111
[19] Abdel Menaem A, Beryozkina S, Safaraliev M. Starting current limiter for three-phase induction motors. In: International Conference on Clean Energy and Electrical Systems, 2024, Singapore: Springer Nature Singapore, pp. 51-61.
[20] Nannen H, Heiko Z, Gerd G. Predictive firing algorithm for soft starter driven induction motors. *IEEE Transactions on Industrial Electronics* 2021; 69:12152–12161. DOI: https://doi.org/10.1109/TIE.2021.3135606
[21] Jang P, Hyon B, Hwang D, Park J, Choi J, Kim J. The seamless transition from discrete frequency control to phase control method using soft starter. *IEEE Access* 2024; 12:13469–13476. DOI: https://doi.org/10.1109/ACCESS.2024.3352635
[22] Solveson MG, Mirafzal B, Demerdash NAO. Soft-started induction motor modeling and heating issues for different starting profiles using a flux linkage ABC frame of reference. *IEEE Trans. Ind. Appl.* 2006; 42:973–982. DOI: https://doi.org/10.1109/TIA.2006.877735

[23] Nied A, Oliveira J, Campos R, Dias R, Marques L. Soft starting of induction motor with torque control. *IEEE Trans. Industry Applications* 2010; 46:1002–1010. DOI: https://doi.org/ 10.1109/TIA.2010.2045335
[24] Zenginobuz G, Çadirci I, Ermis M, Barlak C. Soft starting of large induction motors at constant current with minimized starting torque pulsations. *IEEE Trans. Ind. Appl.* 2001; 37:1334–1347. DOI: https://doi.org/10.1109/28.952509
[25] Sastry VV, Prasad MR, Sivakumar TV. Optimal soft starting of voltage-controller-fed IM drive based on voltage across thyristors. *IEEE Trans. Power Electron.* 1997; 12:1041–1051. DOI: https://doi.org/10.1109/63.641502
[26] Zenginobuz G, Cadirci I, Ermis M, Barlak C. Performance optimization of induction motors during voltage-controlled soft starting. *IEEE Trans. Energy Convers.* 2004; 19:278–288. DOI: https://doi.org/10.1109/TEC.2003.822292
[27] Mohanty M, Sahu SK, Nayak MR, Satpathy A, Choudhury S. Application of Salp Swarm Optimization for PI Controller to Mitigate Transients in a Three-Phase Soft Starter-Based Induction Motor. In: Pradhan G, Morris S, Nayak N, editors. Advances in Electrical Control and Signal Systems. Lecture Notes in Electrical Engineering, vol 665. SINGAPORE: Springer.
[28] Nayak PSR, Rufzal TA. Performance analysis of feedback controller design for induction motor soft-starting using bio-inspired algorithms. In: International Conference on Power, Instrumentation, Control and Computing (PICC); 18-19 Jan. 2020, IEEE, Thrissur, India, pp. 1-6.
[29] Ghadimi M, Ramezani A, Mohammadimehro M. Soft Starter Modeling for an Induction Drive Starting Study in an Industrial Plant. In: UKSim 5th European Symposium on Computer Modeling and Simulation; 16-18 Nov. 2011, IEEE, Madrid, Spain, pp. 245-250.
[30] Çelik E, Gör H, Öztürk N, Kurt E. Application of artificial neural network to estimate power generation and efficiency of a new axial flux permanent magnet synchronous generator. *International Journal of Hydrogen Energy* 2017; 42:17692-17699. DOI: https://doi.org/10.1016/j.ijhydene.2017.01.168
[31] Çelik E, Uzun Y, Kurt E, Öztürk N, Topaloğlu N. A neural network design for the estimation of nonlinear behavior of a magnetically-excited piezoelectric harvester. *Journal of Electronic Materials* 2018; 47:4412-4420. DOI: https://doi.org/10.1007/s11664-018-6078-z
[32] Çelik E. Neural network estimation of mutual inductance variation for a shaded-pole induction motor. *The International Journal of Energy and Engineering Sciences* 2019; 3:36-45.
[33] Faizal A, Subburaj P. Intelligence based soft starting scheme for the three-phase squirrel cage induction motor with extinction angle ac voltage controller. *Circuits and Systems* 2016; 7:2752-2770. DOI: https://doi.org/10.4236/cs.2016.79236
[34] Ze Z, Ming H. Soft starter study of induction motors using fuzzy pid control. *IOP Conference Series: Materials Science and Engineering* 2018; 439:032115. DOI: https://doi.org/10.1088/1757-899X/439/3/032115
[35] Mallick TC, Dhar S, Khan J. Artificial neural network based soft-starter for induction motor. In: 2nd International Conference on Electrical Information and Communication Technologies (EICT); Dec. 2015, Khulna, Bangladesh, pp. 228-233.
[36] Kashif SAR, Saqib MA. A neuro fuzzy application: Soft starting of induction motors with reduced energy losses. *Electr. Power Components Syst.* 2012. DOI: 10.1080/15325008.2012.694970
[37] Hamed SA, Chalmers BJ. Analysis of variable-voltage thyristor-controlled induction motors. *Proc. Inst. Elect. Eng.* 1990; 137:184–193. DOI: https://doi.org/10.1049/IP-B.1990.0019
[38] Abdel Menaem A, Elgamal M, Abdel-Aty AH, Mahmoud EE, Chen Z, Hassan MA. A proposed ANN-based acceleration control scheme for soft starting induction motor. *IEEE Access* 2021; 9:4253-4265. DOI: https://doi.org/10.1109/ACCESS.2020.3046848
[39] Aref M, Abdelmeneam A, Oboskalov V, Mahnitko A, Gavrilov A. Transient analysis of ac and dc microgrid with effective of SFCL. In: IEEE 59th International Scientific Conference on Power and Electrical Engineering of Riga Technical University (RTUCON); Nov. 2018, IEEE, Riga, Latvia, pp. 1-6.
[40] Karanayil B, Rahman MF. Artificial Neural Network Applications in Power Electronics and Electric Drives. In: Muhammad H. Rashidi, editor. *Power Electronics Handbook: Devices, Circuits, and Applications*. Florida, USA: Elsevier, 2018, pp. 1245–1260.